NASA-CR-197317

IN-TERIM
IN-20-CR
39818
P.37

SEMI-ANNUAL STATUS REPORT

Submitted to: NASA Marshall Space Flight Center

Grant Title: THEORY AND COMPUTATION OF OPTIMAL LOW- AND MEDIUM-THRUST TRANSFERS

Grant Number: NAG8-921

Principal Investigator /Project Director: Dr. C.-H. Chuang
School of Aerospace Engineering
Georgia Institute of Technology
Atlanta, GA 30332-0150
Phone: (404) 894-3075
Fax: (404) 894-2760
E-mail: ch.chuang@aerospace.gatech.edu

Research Assistant: Troy D. Goodson
Laura A. Ledsinger
School of Aerospace Engineering
Georgia Institute of Technology

Period Covered: July 7, 1994 to January 6, 1995

Date of Submission: January 5, 1995

(NASA-CR-197317) MULTIPLE BURN FUEL-OPTIMAL ORBIT TRANSFERS: NUMERICAL TRAJECTORY COMPUTATION AND NEIGHBORING OPTIMAL FEEDBACK GUIDANCE Semiannual Status Report, 7 Jul. 1994 - 6 Jan. 1995 (Georgia Inst. of Tech.) 37 p

N95-21616

Unclas

G3/20 0039818

TABLE OF CONTENTS

Multiple Burn Fuel-Optimal Orbit Transfers: Numerical Trajectory Computation and Neighboring Optimal Feedback Guidance

C.-H. Chuang, Troy D. Goodson, and Laura A. Ledsinger
School of Aerospace Engineering
Georgia Institute of Technology, Atlanta, Georgia 30332

ABSTRACT

This report describes current work in the numerical computation of multiple burn, fuel-optimal orbit transfers and presents an analysis of the second variation for extremal multiple burn orbital transfers as well as a discussion of a guidance scheme which may be implemented for such transfers. The discussion of numerical computation focuses on the use of multivariate interpolation to aid the computation in the numerical optimization. The second variation analysis includes the development of the conditions for the examination of both fixed and free final time transfers. Evaluations for fixed final time are presented for extremal one, two, and three burn solutions of the first variation. The free final time problem is considered for an extremal two burn solution. In addition, corresponding changes of the second variation formulation over thrust arcs and coast arcs are included. The guidance scheme discussed is an implicit scheme which implements a neighboring optimal feedback guidance strategy to calculate both thrust direction and thrust on-off times.

I. INTRODUCTION

The necessary conditions which result from analyzing the first variation of a cost functional are widely used. These are commonly referred to as the Euler-Lagrange equations. Many problems require additional considerations, for example, the problem considered herein, fuel-optimal orbit transfer, requires consideration of Pontryagin's Maximum Principle.

Many researchers have used the first variation to compute extremal solutions to the fuel-optimal orbit transfer problem. Some have used them to apply two-point boundary value problem solvers to optimization problems, forming indirect methods.[1,2,3] Others have used a partial set of the conditions to form hybrid indirect/direct methods where certain highly sensitive parameters are optimized directly.[4,5] However, to the knowledge of the authors, few, if any, have made use of the conditions related to the second variation of the cost functional. These provide sufficient conditions which, when met, declare an extremal solution as a local, weak optimal solution.

Once the second variation of the cost functional is verified so that it is known whether the sufficient conditions are met, the information obtained can then be used to implement a guidance scheme. Guidance is defined to be the determination of a way to follow an optimal trajectory when presented with obstacles such as environmental disturbances or uncertainties in navigation data. Two different types of guidance schemes exist: implicit and explicit. Implicit guidance systems are characterized by the fact that the vehicle's motion must be precomputed on the ground and then compared to the actual motion. The equations which need to be solved are based upon the difference between these measured and precomputed values. The solutions to these equations are used in the vehicle's steering and velocity control. Explicit guidance systems are generalized by the fact that the vehicle's equations of motion are modeled and solved for by on-board computers during its motion. The solutions for the equations are solved continuously and are used to determine the difference between the vehicle's current motion and its destination. Commands are then generated to alleviate the anticipated error.

Existing guidance schemes have been presented in various papers. An iterative guidance scheme which is implemented using a linear tangent steering law is presented by Smith.[6] This guidance scheme has been used for the Saturn V and is in currently used by the Space Shuttle, the Atlas-Centaur, and the Titan-Centaur. In a paper by Lu[7], a general nonlinear guidance law is developed using two different strategies. One strategy uses optimal control theory to generate a new optimal trajectory onboard from the start, while the other uses flight-path-restoring-guidance to bring the trajectory back to the nominal. A guidance scheme that is developed using inverse methods for unthrusted, lift-modulated vehicles along an optimal space curve is presented by Hough.[8] Linearized guidance laws applicable to many different types of space missions are presented by Tempelman.[9] These guidance laws are based on fixed and free final time arrivals. Naidu[10] presents a guidance scheme applicable to aeroassisted orbital transfers. This scheme is developed by implementing neighboring optimal guidance and linear quadratic regulator theory. Some interesting techniques for making the neighboring optimal guidance converge about the nominal path are introduced in a paper by Powers.[11]

The guidance scheme proposed in this report is an implicit one which implements neighboring optimal feedback guidance. An implicit guidance system was chosen due to the fact that that type of guidance system handles disturbances well.[10] The neighboring optimal feedback guidance was chosen because it inherently uses the nominal solutions. Also, it has the advantage of being a feedback system, as a opposed to open-loop guidance.

In this scheme, the initial orbit exit point is assumed to be perturbed from the nominal point but the boundary condition, specifying the final orbit, is assumed unchanged. The goal is to use the controller to bring the trajectory back to the nominal path at some point by using minimal fuel.

II. First Variation Considerations

Within this report results are restricted to the planar case, no plane changes are considered at this stage of development. The solutions examined in this report satisfy the conditions related to the first variation. In the next section, the conditions sufficient for declaring a minimizing solution will be checked for these transfers. Some of these transfers are multi-burn transfers and in order to simplify initial analysis new nominal solutions have been constructed from these which are single-burn transfers, i.e. the thrust is kept on for all time between the initial orbit exit point and the final orbit entry point.

Only that part of the original trajectory which is contained in the last burn is taken to constitute the new extremal solution. This new extremal solution has a fixed initial point and fixed transfer time but the final point is only constrained in that it must lie on the final orbit.

II.1. Conditions from the First Variation

The first order conditions for this problem have been stated many times[12] and will be given here only briefly. The optimization problem consists of a cost functional (Eq. [1]), state dynamics (Eqs. [2-4]), fixed initial point conditions (Eq. [5]), and boundary conditions on the terminal point (Eq. [6]); each of these is expressed below.

$$J = -m(t_f) \tag{1}$$

$$\dot{\mathbf{r}} = \mathbf{v} \tag{2}$$

$$\dot{\mathbf{v}} = \frac{T}{m}\mathbf{e}_T - \frac{\mu}{r^3}\mathbf{r} \tag{3}$$

$$\dot{m} = -\frac{T}{g_o I_{sp}} \tag{4}$$

$$\mathbf{r}(t_o) = \mathbf{r}_o, \quad \mathbf{v}(t_o) = \mathbf{v}_o, \quad m(t_o) = m_o \tag{5}$$

$$\begin{bmatrix} \psi_1 \\ \psi_2 \\ \psi_3 \end{bmatrix} = \begin{bmatrix} \mathrm{xv} - \mathrm{yu} \\ (v^2 - \mu/r)\mathrm{x} - (\mathbf{r}^T\mathbf{v})\mathrm{u} \\ (v^2 - \mu/r)\mathrm{y} - (\mathbf{r}^T\mathbf{v})\mathrm{v} \end{bmatrix} - \begin{bmatrix} h \\ \mu e_x \\ \mu e_y \end{bmatrix} \tag{6}$$

where $\mathbf{r}=[\mathrm{x}\ \mathrm{y}]^{\mathrm{T}}$ is the radius vector, $\mathrm{v}=[\mathrm{u}\ \mathrm{v}]^{\mathrm{T}}$ is its time derivative, $\mathbf{e}_T$ is the thrust direction, a unit vector, T is thrust magnitude (limited between zero and some maximum value T_{max}), μ is the gravitational constant, g_o is the gravitational acceleration at sea-level, I_{sp} is the specific impulse of the motor. The quantity $g_o I_{sp}$ is often referred to as the exit velocity of the motor. The Euler Lagrange conditions are then

$$\mathbf{e}_T = \frac{-\boldsymbol{\lambda}_v}{|\boldsymbol{\lambda}_v|} \tag{7}$$

$$\dot{\boldsymbol{\lambda}}_r = \mu\left[\frac{\boldsymbol{\lambda}_v}{r^3} - 3\frac{(\boldsymbol{\lambda}_v{}^T\mathbf{r})\mathbf{r}}{r^5}\right] \tag{8}$$

$$\dot{\boldsymbol{\lambda}}_v = -\boldsymbol{\lambda}_r \tag{9}$$

$$\dot{\lambda}_m = \frac{T}{m^2}\boldsymbol{\lambda}_v{}^T\mathbf{e}_T = \frac{T}{m^2}|\boldsymbol{\lambda}_v| \tag{10}$$

where $\boldsymbol{\lambda}_r=[\lambda_x\ \lambda_y]^T$ and $\boldsymbol{\lambda}_v=[\lambda_u\ \lambda_v]^T$. The natural boundary conditions are

$$\lambda_x(t_f) = \nu_3 \mathrm{v} + \nu_4(\mathrm{v}^2 - \mu/r + \mu \mathrm{x}^2/r^3) + \nu_5(\mu \mathrm{xy}/r^3 - \mathrm{uv})\Big|_{t=t_f} \tag{11}$$

$$\lambda_y(t_f) = -\nu_3 \mathrm{u} + \nu_4(\mu \mathrm{xy}/r^3 - \mathrm{uv}) + \nu_5(\mathrm{u}^2 - \mu/r + \mu \mathrm{y}^2/r^3)\Big|_{t=t_f} \tag{12}$$

$$\lambda_u(t_f) = -\nu_3 \mathrm{y} - \nu_4 \mathrm{yv} + \nu_5(2\mathrm{yu} - \mathrm{xv})\Big|_{t=t_f} \tag{13}$$

$$\lambda_v(t_f) = \nu_3 \mathrm{x} + \nu_4(2\mathrm{xv} - \mathrm{uy}) - \nu_5 \mathrm{xu}\Big|_{t=t_f} \tag{14}$$

$$\lambda_m(t_f) = -1 \tag{15}$$

The conditions resulting from applying Pontryagin's Minimum Principle are

$$
\begin{aligned}
H_S < 0, \quad T = T_{max} \\
H_S > 0, \quad T = 0
\end{aligned}
\tag{16}
$$

where

$$
H_S = -\left(\frac{|\lambda_v|}{m} + \frac{\lambda_m}{g_o I_{sp}} \right)
\tag{17}
$$

Note that when the derivatives of H_S are zero, singular arc solutions may exist. This has been checked numerically.[12]

Finally, the free final time problem will also be considered here. For these extremal solutions the final, or transfer, time is selected such that the transversality condition is satisfied, i.e. the Hamiltonian is zero at $t=t_f$.

$$
H(t_f) = \lambda_r^T \dot{\mathbf{r}} + \lambda_v^T \dot{\mathbf{v}} \Big|_{t=t_f} = 0
\tag{18}
$$

In a previous paper[12] this problem was given as a maximization problem. To conform to the convention used for the second variation[13], it is now stated as a minimization problem. If an extremal solution to the maximization problem is given as state time history $\mathbf{x}(t)$, Lagrange-multiplier time history $\lambda(t)$, and Lagrange multipliers ν, associated with boundary conditions, then the extremal solution of the above minimization problem is $\mathbf{x}(t)$, $(-1)*\lambda(t)$, and $(-1)*\nu$.

Additionally, it makes more sense in the guidance problem to consider the control as the angle θ, rather than individual components of a unit vector. This simplifies analysis because the control is now a scalar. Equation [7] must now be restated as

$$
tan(\theta) = -\frac{\lambda_v}{\lambda_u}
\tag{19}
$$

II.2. EXTREMAL SOLUTIONS

All quantities associated with the solutions presented here have been nondimensionalized so that $\mu=1$ and will be presented here in that form. The relations used to nondimensionalize are given below.

$$\hat{\mathbf{r}} \equiv \frac{\mathbf{r}}{r^\star} \qquad \hat{\mathbf{v}} \equiv \frac{\mathbf{v}}{\sqrt{\mu/r^\star}} \tag{20-21}$$

$$\hat{m} \equiv \frac{m}{m^\star} \qquad \hat{t}_f \equiv \frac{t_f}{\sqrt{(r^\star)^3/\mu}} \tag{22-23}$$

$$\hat{T} \equiv \frac{T/m^\star}{\mu/(r^\star)^2} \qquad \left(\hat{g}_o \hat{I}_{sp}\right) = g_o I_{sp} \sqrt{r^\star/\mu} \tag{24-25}$$

where $r^\star$ and $m^\star$ are indicated in the tables for each case of the extremal solutions.

Each of the transfers given below have both the initial orbit exit point and final orbit entry points free. However, for the guidance problem it makes more physical sense to consider the initial orbit exit point as fixed and equal to the optimal choice, for it cannot be updated once the transfer has begun.

The last burn of any multi-burn transfer below may also be taken as a complete transfer unto itself. The initial point can be chosen as the one at the very first instant (or shortly thereafter) of thrusting for the last burn. The final orbit exit point must remain unchanged. Obviously, for these choices the natural boundary conditions for final orbit entry point are still satisfied. This new transfer can then be considered as a new extremal solution, though to an orbit transfer problem with a different initial orbit.

Figure 1 shows a one burn ascent extremal solution. This trajectory is a transfer leaving an orbit with a semimajor axis a=1.069, eccentricity e=0.02633, and argument of perigee ω= -50°. The transfer ends at a nearby orbit with a=1.038 and e=0. Other pertinent transfer data are given in Table I. This transfer was produced by shortening the time of a two-burn transfer until the coast arc between them vanished. This transfer is therefore both a minimum mass and minimum time extremal solution because mass and time have an affine relationship in the one-burn case.

Figure 2 displays a two-burn transfer, in fact a descending transfer, from an orbit with elements a=3.847, e=0.02378 to a final orbit with elements a=1.5, e=0.3333. The apses of the terminal orbits are aligned and lie on the 'X' axis of the figure. The initial mass is 1.608 and the final mass is 1.1547. Other pertinent transfer data are given in Table II. This transfer has the transversality condition converged, therefore it is a candidate fuel-optimal free final time solution. By the same right, it can also be considered a candidate optimal solution for the fixed final time problem.

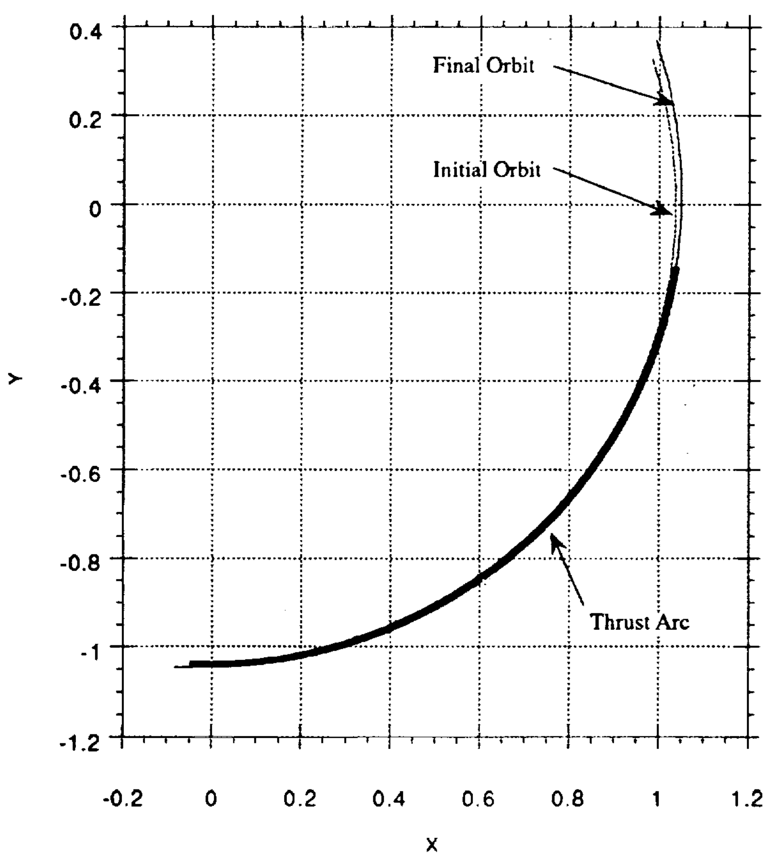

Figure 1: One-Burn Extremal with Fixed Final Time.

$g_o J_{sp}=$	0.3861	$a_i=$	1.038	$\omega_i=$	n/a	$a_f=$	1.069	$\omega_f=$	-50°
$T=$	0.03	$e_i=$	0.000	$t_f=$	1.553	$e_f=$	0.02633	$m_f=$	1.542
$r^☆=$	6378 *km*	$m^☆=$	14 *Mg*						

Table I. Parameters of the Transfer Shown in Figure 1.

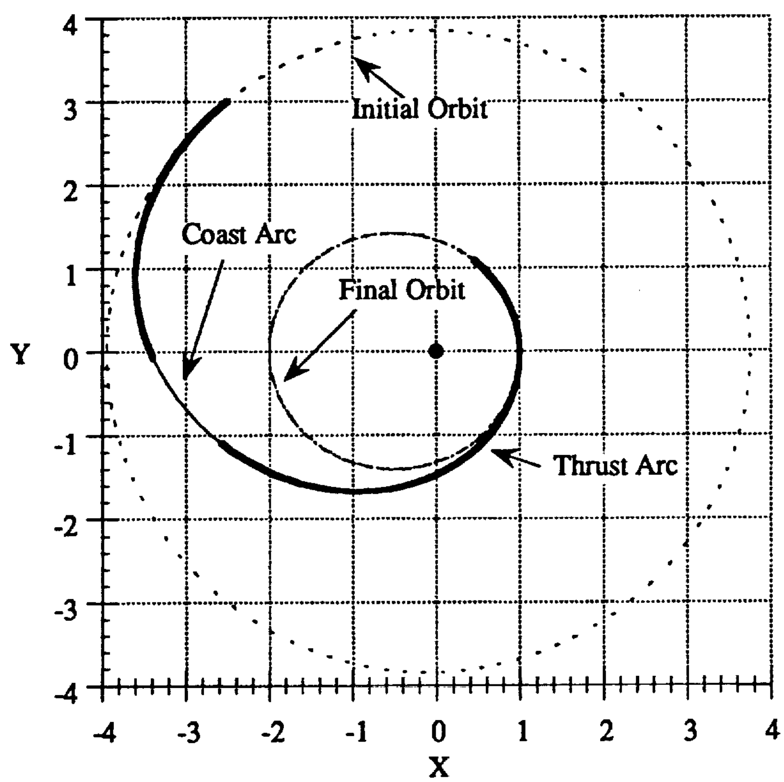

Figure 2: Two-Burn Extremal Orbit Transfer Solution with Free Final Time.

$g_o J_{sp}=$	1.313	$a_i=$	3.847	$\omega_i=$	0°	$a_f=$	1.5	$\omega_f=$	0°
$T=$	0.03	$e_i=$	0.02378	$t_f=$	19.05	$e_f=$	0.3333	$m_f=$	1.608
$r^☆=$	6878 *km*	$m^☆=$	200 *kg*						

Table II Parameters of Transfer in Figure 2.

A three-burn transfer is shown in Figure 3. Since this transfer is between orbits of increasing semimajor axis, it will be referred to as an ascending transfer. The initial orbit has elements a=2.239, e=0.1160, and ω=-85.94°. The elements of the final orbit are a=7, e=0.7332, and w=114.6°. Other pertinent transfer data are given in Table III.

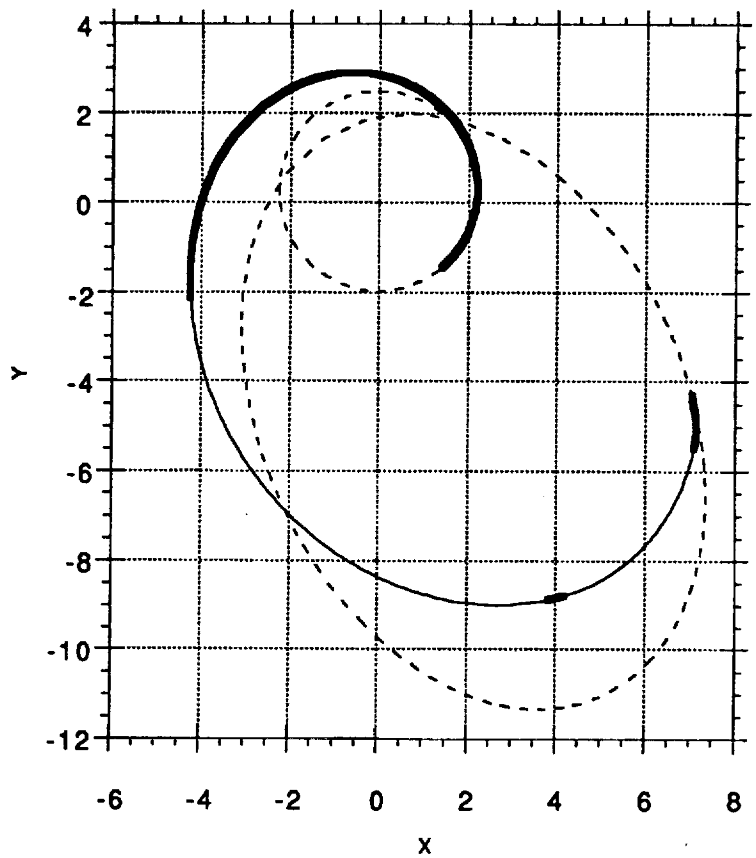

Figure 3: **Three-Burn Extremal Orbit Transfer with Fixed Final Time.**

$g_0 I_{sp}$ =	0.3898	a_i=	2.239	ω_i=	-85.94°	a_f=	7.000	ω_f=	114.6°
T=	0.01386	e_i=	0.1160	t_f=	85.00	e_f=	0.7332	m_f=	0.6056
$r^{\star}$=	6378 *km*	$m^{\star}$=	14 *Mg*						

Table III. **Parameters of the transfer shown in Figure 3.**

III. CHECKING THE SECOND VARIATION

Extensive derivation of the conditions for the second variation of the cost functional has already been detailed in Ref [13]. Equations given in this section are the results of applying this work to our problem.

Considering the second variation of the augmented cost functional, J, a new optimal control problem can be stated. In this new problem, the state is δx, the control δu, and the Lagrange-multipliers are $\delta\lambda$ and dv.. Thus the new cost function is

$$\delta^2\bar{J} = \frac{1}{2}\left[\delta x^T\left(\phi_{xx} + \left(v^T\psi_x\right)_x\right)\delta x\right]_{t=t_f} + \frac{1}{2}\int_{t_o}^{t_f}\left[\delta x^T \quad \delta u^T\right]\begin{bmatrix} H_{xx} & H_{xu} \\ H_{ux} & H_{uu} \end{bmatrix}\begin{bmatrix} \delta x \\ \delta u \end{bmatrix} dt \tag{26}$$

subject to

$$\delta\dot{x} = f_x\delta x + f_u\delta u \tag{27}$$

$$\delta x(t_o) = \delta x_o \tag{28}$$

where $x=[r^T\ v^T\ m]^T$ and $u=\theta$.

In general, neighboring optimal feedback guidance allows the designer to consider changes in final boundary conditions. We consider no such changes, assuming that the destination orbit was accurately planned well in advance. Formulation will be made below for both the fixed and free final time cases.

Evaluating the terms in Eq. [26-28], for orbital transfer, the partial derivatives for the dynamics and for the Hamiltonian are:

$$\mathbf{f}_x = \begin{bmatrix} 0 & 0 & 1 & 0 & 0 \\ 0 & 0 & 0 & 1 & 0 \\ -\left(\frac{\mu}{r^3}\right) - \frac{3\mu x^2}{r^5} & \frac{3\mu xy}{r^5} & 0 & 0 & -\frac{T}{m}\cos(\theta) \\ \frac{3\mu xy}{r^5} & -\left(\frac{\mu}{r^3}\right) - \frac{3\mu y^2}{r^5} & 0 & 0 & -\frac{T}{m}\sin(\theta) \\ 0 & 0 & 0 & 0 & 0 \end{bmatrix} \tag{29}$$

$$
\mathbf{f}_{\theta} = \begin{bmatrix} 0 \\ 0 \\ -\frac{T}{m} sin(\theta) \\ \frac{T}{m} cos(\theta) \\ 0 \end{bmatrix} \tag{30}
$$

$$
\mathbf{H}_{xx} = \begin{bmatrix} -\mu\left(\frac{-3(3\lambda_u x + \lambda_v y)}{r^5} + \frac{15(\lambda_v^T r)x^2}{r^7}\right) & -\mu\left(\frac{-3(\lambda_u y + \lambda_v x)}{r^5} + \frac{15(\lambda_v^T r)xy}{r^7}\right) & 0 & 0 & 0 \\ -\mu\left(\frac{-3(\lambda_u y + \lambda_v x)}{r^5} + \frac{15(\lambda_v^T r)xy}{r^7}\right) & -\mu\left(\frac{-3(3\lambda_v y + \lambda_u x)}{r^5} + \frac{15(\lambda_v^T r)y^2}{r^7}\right) & 0 & 0 & 0 \\ 0 & 0 & 0 & 0 & 0 \\ 0 & 0 & 0 & 0 & 0 \\ 0 & 0 & 0 & 0 & 2\frac{T}{m^3}|\lambda_v| \end{bmatrix} \tag{31}
$$

$$
H_{\theta\theta} = \frac{T}{m}|\lambda_v| \tag{32}
$$

$$
H_{\theta x} = 0 \tag{33}
$$

The fixed and free final time problems have the following equations in common:

$$
\delta\dot{x} = \mathbf{A}(t)\delta\mathbf{x} - \mathbf{B}(t)\delta\lambda \tag{34}
$$

$$
\delta\dot{\lambda} = -C(t)\delta\mathbf{x} - \mathbf{A}^T(t)\delta\lambda \tag{35}
$$

where

$$
\mathbf{A}(t) = \mathbf{f}_x - \mathbf{f}_u H_{uu}^{-1}\mathbf{H}_{ux} \tag{36}
$$

$$
\mathbf{B}(t) = \mathbf{f}_u H_{uu}^{-1}\mathbf{f}_u^T \tag{37}
$$

$$
C(t) = \mathbf{H}_{xx} - \mathbf{H}_{xu}H_{uu}^{-1}\mathbf{H}_{ux} \tag{38}
$$

For a multiple-burn solution, one finds that $H_{\theta\theta}$ becomes zero during coast arcs. This makes it impossible to solve for the change in control, $\delta\theta$. However, since the thrust is off during a coast arc, it physically makes no difference what choice is made for the control. Therefore, $\delta\theta$ may be chosen as zero and simpler expressions for $\mathbf{A}(t)$, $\mathbf{B}(t)$, and $\mathbf{C}(t)$ can be written as

$$\mathbf{A}(t) = \mathbf{f}_x \tag{39}$$

$$\mathbf{B}(t) = 0 \tag{40}$$

$$\mathbf{C}(t) = \mathbf{H}_{xx} \tag{41}$$

Using the sweepback method for nonlinear terminal constraints, as is the case for this development, the form for $\delta\lambda$ and $\delta\psi$ are assumed as

$$\delta\lambda(t) = \mathbf{P}(t)\delta x(t) + \mathbf{S}(t)d\nu \tag{42}$$

$$\delta\psi = \mathbf{S}^{T}(t)\delta x(t) + \mathbf{V}(t)d\nu \tag{43}$$

which allows the solution for $d\nu$ to be written as

$$d\nu = \mathbf{V}^{-1}(t_o)\left[\delta\psi - \mathbf{S}^{T}(t_o)\delta x(t_o)\right] \tag{44}$$

As mentioned above, $\delta\psi=0$ will be considered here. The boundary condition equations are given by:

$$\mathbf{P}(t_f) = \left[\phi_{xx} + \left(\nu^{T}\psi_x\right)_x\right]_{t=t_f} \tag{48}$$

$$S(t_f) = \left[\psi_x^T\right]_{t=t_f} \tag{49}$$

$$V(t_f) = 0 \tag{50}$$

where in the development for the orbital transfer these are:

$$P(t_f) = \begin{bmatrix} a & b & d & e & 0 \\ b & c & f & g & 0 \\ d & f & h & i & 0 \\ e & g & i & j & 0 \\ 0 & 0 & 0 & 0 & 0 \end{bmatrix} \tag{51}$$

where

$$a = \nu_2\mu\left[\frac{x(t_f)}{R^3} - \frac{3x^3(t_f)}{R^5} + \frac{2x(t_f)}{R^3}\right] + \nu_3\mu\left[\frac{y(t_f)}{R^3} - \frac{3x^2(t_f)y(t_f)}{R^5}\right] \tag{52a}$$

$$b = \nu_2\mu\left[\frac{y(t_f)}{R^3} - \frac{3x^2(t_f)y(t_f)}{R^5}\right] + \nu_3\mu\left[\frac{x(t_f)}{R^3} - \frac{3x(t_f)y^2(t_f)}{R^5}\right] \tag{52b}$$

$$c = \nu_3\mu\left[\frac{y(t_f)}{R^3} - \frac{3y^3(t_f)}{R^5} + \frac{2y(t_f)}{R^3}\right] + \nu_2\mu\left[\frac{x(t_f)}{R^3} - \frac{3x(t_f)y^2(t_f)}{R^5}\right] \tag{52c}$$

$$d = -\nu_3 v(t_f) \tag{52d}$$

$$e = \nu_1 - \nu_2 u(t_f) + 2\nu_3 v(t_f) \tag{52e}$$

$$f = -\nu_1 - \nu_2 v(t_f) + 2\nu_3 u(t_f) \tag{52f}$$

$$g = -\nu_2 u(t_f) \tag{52g}$$

$$h = 2\nu_3 y(t_f) \tag{52h}$$

$$i = -\nu_3 x(t_f) - \nu_2 y(t_f) \tag{52i}$$

$$j = 2\nu_2 x(t_f) \tag{52j}$$

$$
S(t_f) = \begin{bmatrix} v(t_f) & v^2(t_f) - \frac{\mu}{R} + \frac{\mu x^2(t_f)}{R^3} & \frac{x(t_f)y(t_f)}{R^3} - u(t_f)v(t_f) \\ -u(t_f) & \frac{x(t_f)y(t_f)}{R^3} - u(t_f)v(t_f) & u^2(t_f) - \frac{\mu}{R} + \frac{\mu y^2(t_f)}{R^3} \\ -y(t_f) & -y(t_f)v(t_f) & 2y(t_f)u(t_f) - x(t_f)v(t_f) \\ x(t_f) & 2x(t_f)v(t_f) - u(t_f)y(t_f) & -x(t_f)u(t_f) \\ 0 & 0 & 0 \end{bmatrix} \tag{53}
$$

Following from the assumptions expressed as Eqs. [46-47], the following nonlinear equations for **P**, **S**, and **V** must be integrated backwards. The results will be used to check the sufficient conditions governing a minimizing solution.

$$
\dot{\mathbf{P}} = -\mathbf{PA} - \mathbf{A}^T\mathbf{P} + \mathbf{PBP} - \mathbf{C} \tag{54}
$$

$$
\dot{\mathbf{S}} = -\left(\mathbf{A}^T - \mathbf{PB}\right)\mathbf{S} \tag{55}
$$

$$
\dot{\mathbf{V}} = \mathbf{S}^T\mathbf{BS} \tag{56}
$$

To satisfy the sufficient conditions, $H_{\theta\theta}$, **P**, **S**, and **V** must be such that

$$
\text{convexity condition: } H_{\theta\theta}(t) > 0 \text{ for } t_o \le t \le t_f \tag{57}
$$

$$
\text{normality condition: } \mathbf{V}^{-1}(t) \text{ exists for } t_o \le t < t_f \tag{58}
$$

$$
\text{conjugate point condition: } \mathbf{P}(t) - \mathbf{S}(t)\mathbf{V}^{-1}(t)\mathbf{S}^T(t) \text{ finite for } t_o \le t < t_f \tag{59}
$$

The convexity condition is satisfied for any transfer satisfying the choice of control specified by the Euler-Lagrange equations. This can be seen by noting that Eq.[32] is positive definite, irrespective of the time history for the Lagrange multipliers.

III.1. NUMERICAL RESULTS FOR FIXED FINAL TIME

The results discussed in this section were obtained for nominal solutions with fixed transfer time. The eigenvalues of the V(t) matrix are plotted in Figure 4 for the 3-burn extremal solution. Note that V(t) is not negative definite, one of the eigenvalues is zero for all time and the other two eigenvalues are positive. Therefore, the normality condition is violated. Furthermore, the conjugate point condition cannot be checked. It must be concluded that the 3-burn extremal does not satisfy the sufficient conditions and cannot be considered an optimal solution for fixed final time. Figure 5 shows the eigenvalues of V(t) over the one-burn extremal constructed from this solution in the manner described earlier. The same conclusions must be made for this transfer.

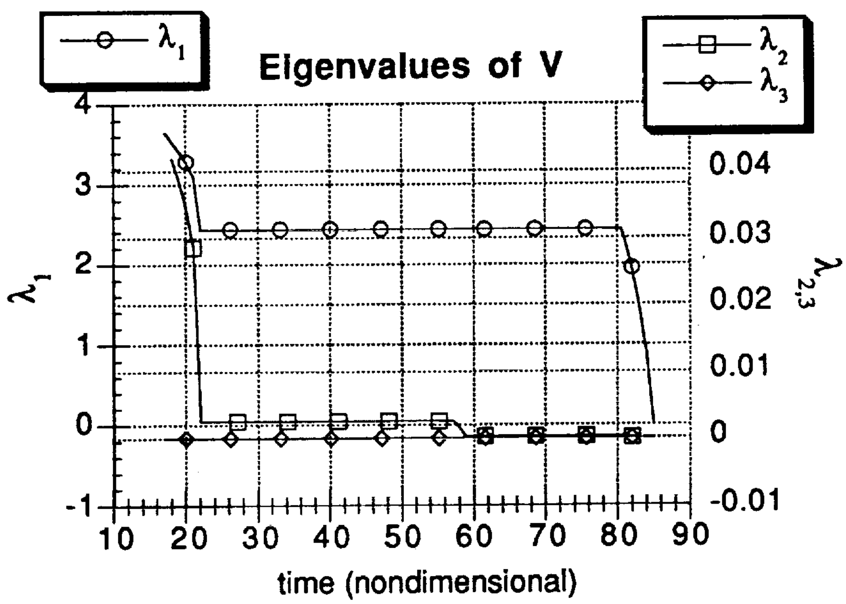

Figure 4: Plot of Eigenvalues of V(t) for Three Burn Extremal.

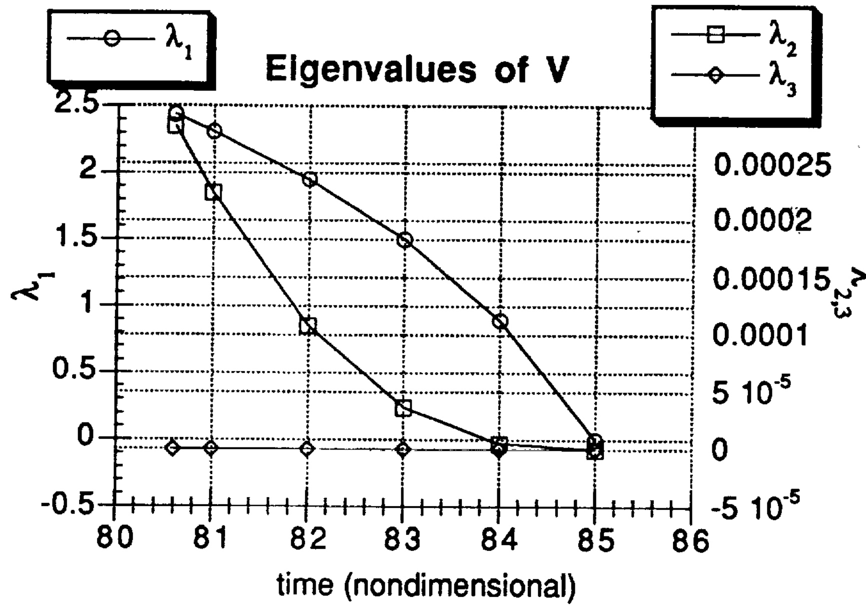

Figure 5: Plot of Eigenvalues of V(t) for Last Burn of Three-Burn Extremal.

The eigenvalues of V(t) for the single-burn transfer are shown in Figure 6. This plot is again made for the two-burn extremal in Figure 7 and a one-burn constructed from it in Figure 8. These figures all show similar results, namely that V(t) is not negative definite, but positive semidefinite. The situation has been repeated, namely that the normality condition has been violated and the conjugate point condition cannot be checked. Therefore, none of the extremal solutions with fixed final time given in this report satisfy the sufficient conditions for a minimizing solution.

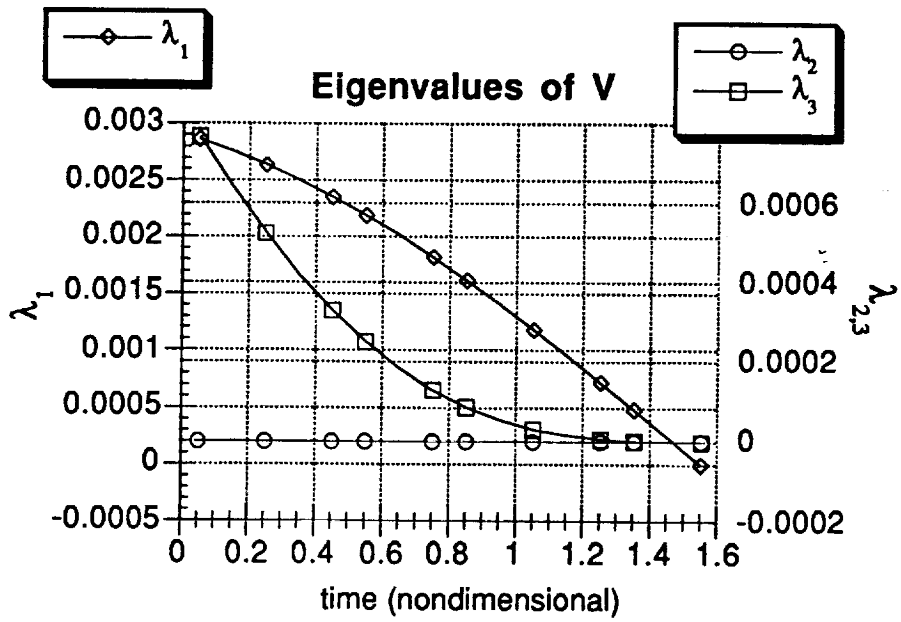

Figure 6: **Plot of Eigenvalues for One-Burn Extremal.**

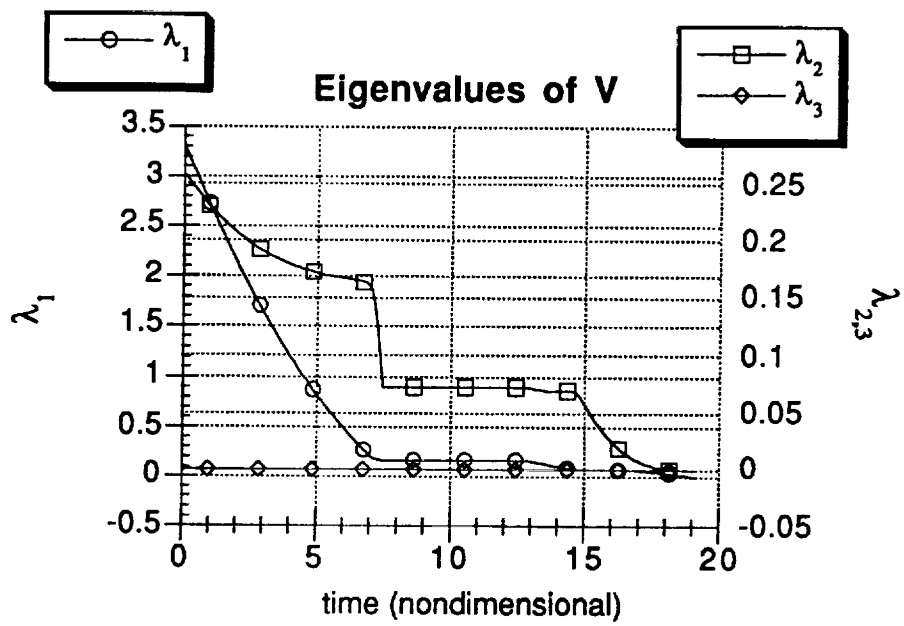

Figure 7: **Plot of Eigenvalues of V(t) for Two-Burn Extremal.**

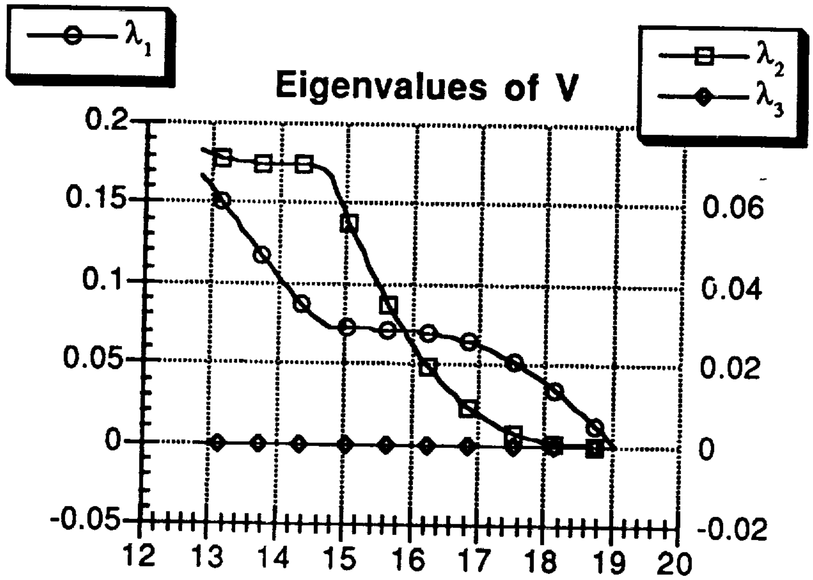

Figure 8: Plot of Eigenvalues of V(t) for Last Burn of Two-Burn Extremal.

III.2. NUMERICAL RESULTS FOR FREE FINAL TIME

When the final time is unspecified, a new condition, the transversality condition, must be satisfied by the nominal solution. This condition is expressed in Eq. [60a]

$$\Omega(\mathbf{x},\mathbf{u},\nu,t)\big|_{t=t_f} \equiv \left(\frac{d\Phi}{dt}+\mathbf{L}\right)_{t=t_f} = 0 \tag{60a}$$

$$\text{where } \Phi = \phi(\mathbf{x},t) + \nu^T\psi(\mathbf{x},t) \tag{60b}$$

$$\frac{d\Phi}{dt} = \frac{\partial\Phi}{\partial t} + \frac{\partial\Phi}{\partial \mathbf{x}}\dot{\mathbf{x}} \tag{60c}$$

This slightly complicates the process of checking the sufficient conditions. The sweepback method can be used with some additions. Three differential equations and thus three boundary conditions must be added to those for **P**, **S**, and **V**.

$$\dot{\mathbf{m}} = -\left(\mathbf{A}^T - \mathbf{PB}\right)\mathbf{m}, \qquad \mathbf{m}(t_f) = \left(\frac{d\Omega}{d\mathbf{x}}\right)^T_{t=t_f} \tag{61}$$

$$\dot{\mathbf{n}} = \mathbf{S}^T\mathbf{B}\mathbf{m}, \qquad \mathbf{n}(t_f) = \left(\frac{d\psi}{dt}\right)_{t=t_f} \tag{62}$$

$$\dot{\alpha} = \mathbf{m}^T\mathbf{B}\mathbf{m}, \qquad \alpha(t_f) = \left(\frac{d\Omega}{dt}\right)_{t=t_f} \tag{63}$$

These additions are used to form $\overline{\mathbf{P}}$, $\overline{\mathbf{S}}$, and $\overline{\mathbf{V}}$ matrices as follows:

$$\overline{\mathbf{P}} = \mathbf{P} - \frac{\mathbf{m}\mathbf{m}^T}{\alpha} \tag{64}$$

$$\overline{\mathbf{S}} = \mathbf{S} - \frac{\mathbf{m}\mathbf{n}^T}{\alpha} \tag{65}$$

$$\overline{\mathbf{V}} = \mathbf{V} - \frac{\mathbf{n}\mathbf{n}^T}{\alpha} \tag{66}$$

The equations for $d\nu$ and $\delta\lambda$ change by substituting $\overline{\mathbf{P}}$, $\overline{\mathbf{S}}$, and $\overline{\mathbf{V}}$ for $\mathbf{P}$, $\mathbf{S}$, and $\mathbf{V}$ respectively, giving

$$d\nu = \overline{\mathbf{V}}^{-1}(t_o)\left[\delta\psi - \overline{\mathbf{S}}^{t}(t_o)\delta\mathbf{x}(t_o)\right] \tag{67}$$

$$\delta\lambda(t) = \overline{\mathbf{P}}(t)\delta\mathbf{x}(t) + \overline{\mathbf{S}}(t)d\nu \tag{68}$$

Note again, however that $\delta\psi$ has been assumed zero. Now, the sufficient conditions based on the second variation with free final time are:

convexity condition: $H_{\theta\theta}(t) > 0$ for $t_o \le t \le t_f$ (69)

normality condition:
$\overline{\mathbf{V}}^{-1}(t)$ exists for $t_o \le t < t_f$ (70a)
$\alpha^{-1}(t)$ exists for $t_o \le t < t_f$ (71b)

conjugate point condition: $\overline{\mathbf{P}}(t) - \overline{\mathbf{S}}(t)\overline{\mathbf{V}}^{-1}(t)\overline{\mathbf{S}}^T(t)$ finite for $t_o \le t < t_f$ (72)

The eigenvalues of $\overline{\mathbf{V}}$ are plotted in Figure 9. Figures 10-12 plot the elements of the conjugate point condition matrix. Figure 13 is a plot of $\alpha(t)$. Figure 9 shows that $\overline{\mathbf{V}}$ is positive definite in the required interval. Figure 13 shows that $\alpha(t)$ is negative definite in the required interval. Since the normality condition requires that the inverse of $\overline{\mathbf{V}}$ and $\alpha(t)$ exists in the interval, this solution is normal. Figures 10-12 show that the conjugate point condition is satisfied. The elements are bounded in the required interval and grow asymptotically at the final time. Therefore, this solution satisfies the sufficient conditions for minimizing the cost functional with free transfer time.

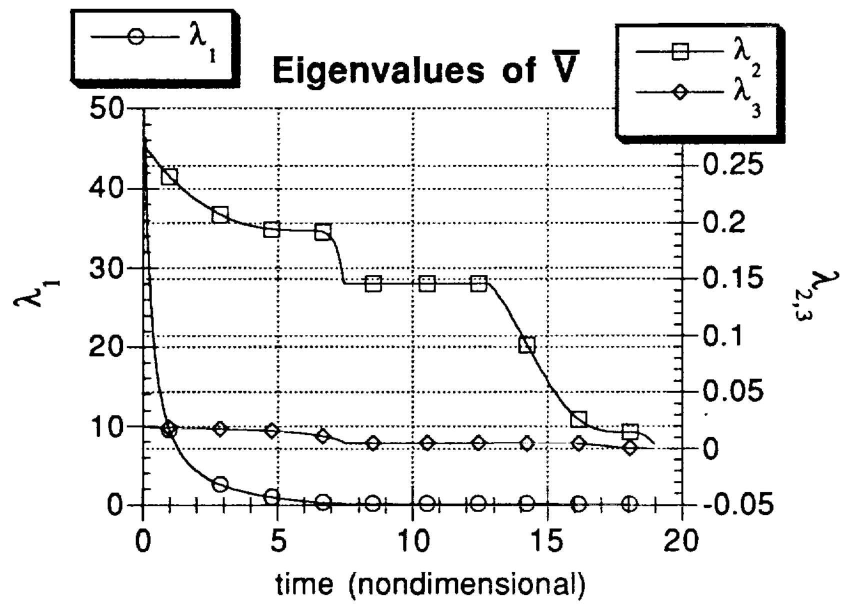

Figure 9 **Plot of Eigenvalues of $\overline{\mathbf{V}}(t)$ for Two Burn Extremal.**

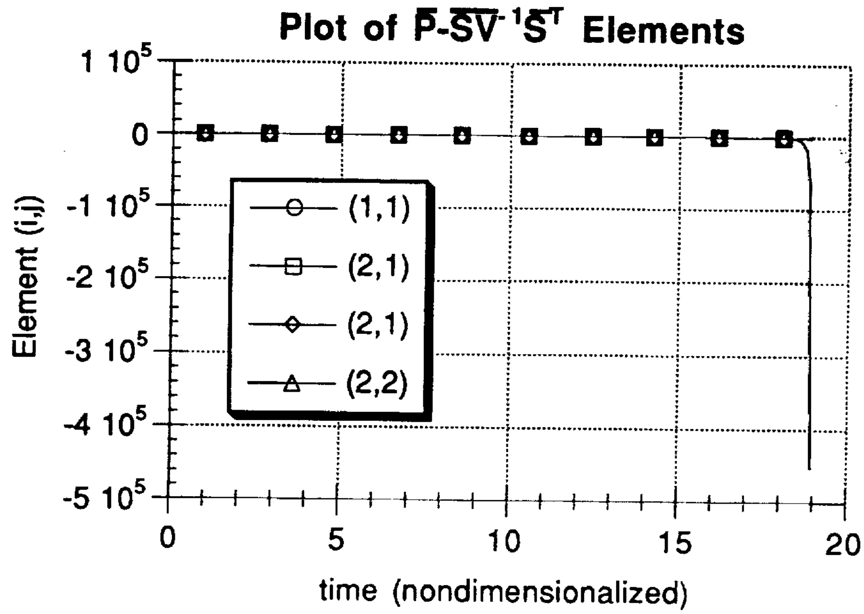

Figure 10: **Plot of Elements of Conjugate Point Condition Matrix for Two Burn Extremal.**

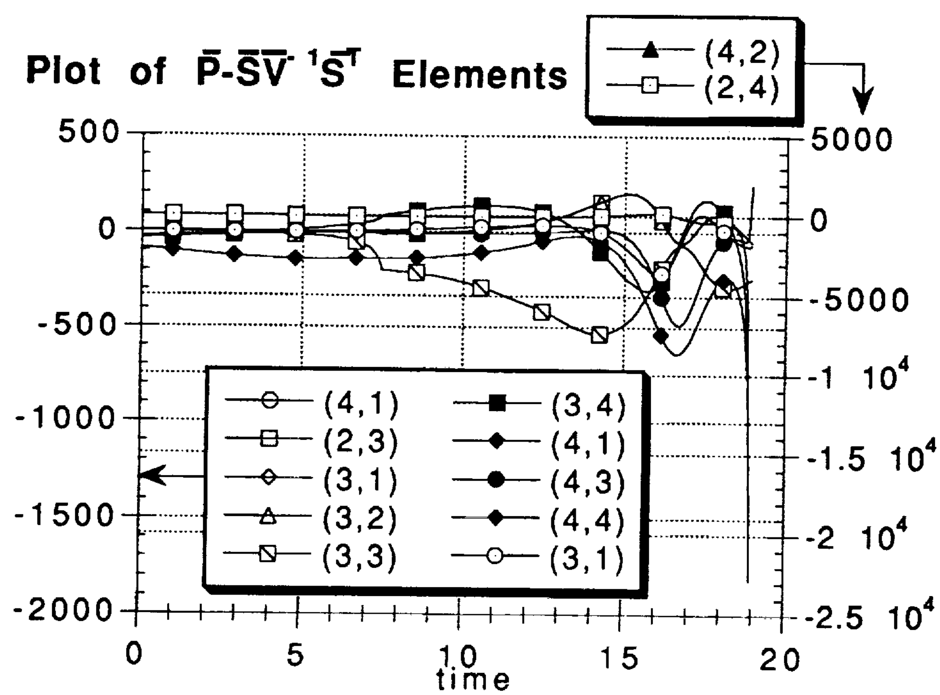

Figure 11: **Plot of Elements of Conjugate Point Condition Matrix for Two Burn Extremal.**

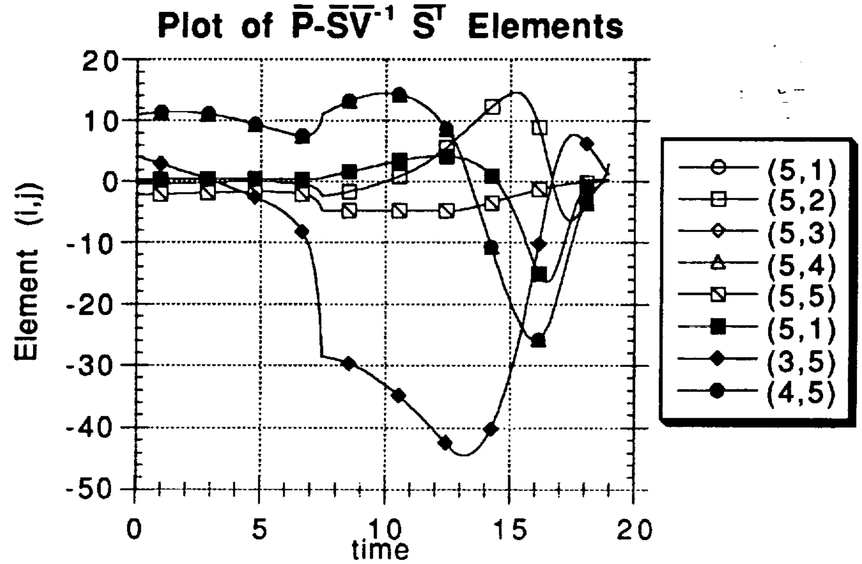

Figure 12: Plot of Elements of Conjugate Point Condition Matrix for Two Burn Extremal.

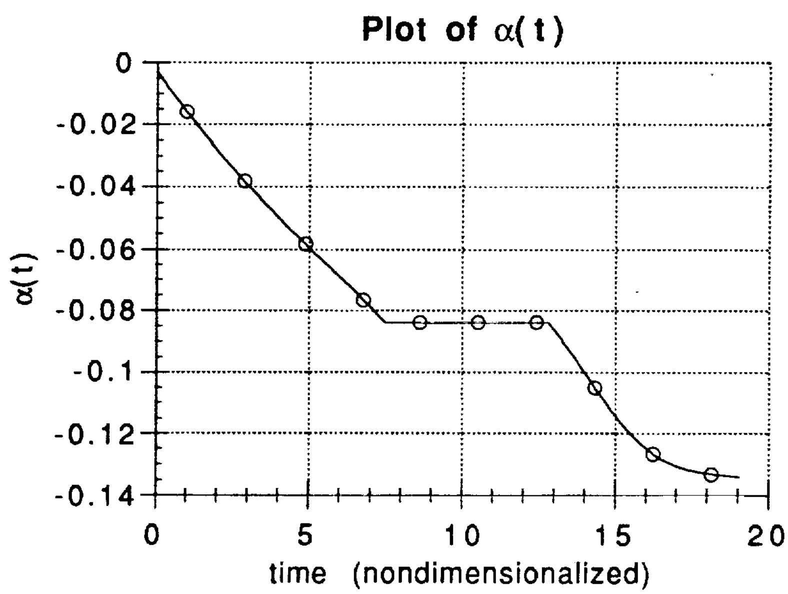

Figure 13: Plot of $\alpha(t)$ for Two Burn Extremal.

Numerical results were also obtained for a one burn case using the same free final time solution. Figs. 14 & 15 show that the normality condition is indeed met in that, respectively, $\alpha(t)$ exists and $\overline{V}^{-1}$ exists

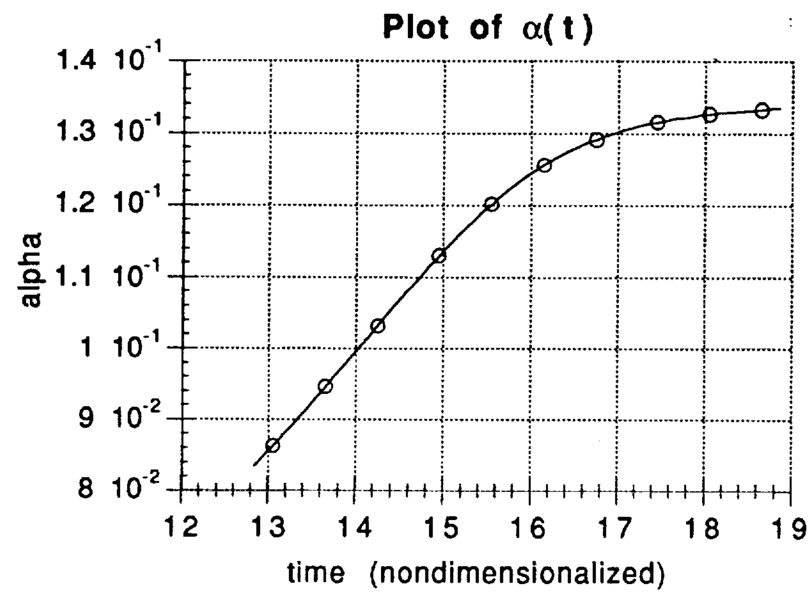

Figure 14: **Plot of $\alpha(t)$ for One Burn Extremal.**

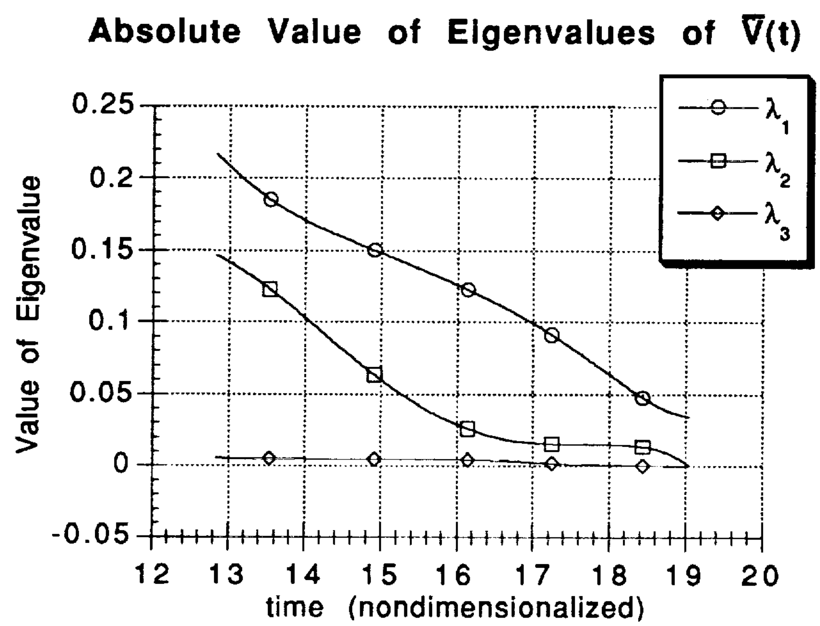

Figure 15: **Plot of Eigenvalues of $\overline{V}$ for One Burn Extremal.**

As seen above in Figs. 10-12, the conjugate point condition is met for the two burn case in that the elements of the matrix required for that condition are finite; thus the conditions can be met similarly for the one burn case for the same solution.

IV. Neighboring Optimal Feedback Guidance

Conveniently, construction of a neighboring optimal feedback guidance law uses the same information as that required to check the second variation of the cost functional. As a result, much of the derivation required of guidance law has been stated already. The remaining discussion will describe how to form the feedback control law and adjust the characteristics of the bang-bang control in a feedback law.

The control, $\delta\theta$, for the fixed final time problem can be found using

$$\begin{aligned} \delta\theta(\mathrm{t}) &= -\mathrm{H}_{\theta\theta}^{-1}\left[\left(\mathbf{f}_{\mathrm{u}}^{\mathrm{T}}\mathbf{P}\right)\delta\mathbf{x} + \mathbf{f}_{\mathrm{u}}^{\mathrm{T}}\mathbf{S}d\mathrm{v}\right] \\ &= -\mathrm{H}_{\theta\theta}^{-1}\left[\mathbf{f}_{\mathrm{u}}^{\mathrm{T}}\left(\mathbf{P} - \mathbf{S}\mathbf{V}^{-1}\mathbf{S}^{T}\right)\right]\delta\mathbf{x} \end{aligned} \tag{73}$$

Note that this continuous feedback law has been constructed by estimating $d\mathrm{v}$ at each instant of time. The feedback law depends on **P**, **S**, and **V** as functions of time. A particular advantage of the sweepback method is the solution of $P(t_0)$, $S(t_0)$, and $V(t_0)$, allowing the guidance law to store these values and propagate them forward to the current time to calculate the current feedback gain. Propagation of the feedback gain may be by integration or more practically by interpolation between stored values. Use of this control should keep the trajectory on a neighboring optimal solution and deliver the spacecraft to the required orbit in the specified transfer time.

If the transfer time is not fixed, and was chosen optimally for the nominal trajectory. Then the formulation for free final time as stated earlier can be used to obtain the feedback guidance law

As seen above in Figs. 10-12, the conjugate point condition is met for the two burn case in that the elements of the matrix required for that condition are finite; thus the conditions can be met similarly for the one burn case for the same solution.

IV. Neighboring Optimal Feedback Guidance

Conveniently, construction of a neighboring optimal feedback guidance law uses the same information as that required to check the second variation of the cost functional. As a result, much of the derivation required of guidance law has been stated already. The remaining discussion will describe how to form the feedback control law and adjust the characteristics of the bang-bang control in a feedback law.

The control, $\delta\theta$, for the fixed final time problem can be found using

$$\begin{aligned} \delta\theta(t) &= -H_{\theta\theta}^{-1}\left[\left(\mathbf{f}_u^T\mathbf{P}\right)\delta x + \mathbf{f}_u^T\mathbf{S}\,d\nu\right] \\ &= -H_{\theta\theta}^{-1}\left[\mathbf{f}_u^T\left(\mathbf{P} - \mathbf{S}\mathbf{V}^{-1}\mathbf{S}^T\right)\right]\delta x \end{aligned} \tag{73}$$

Note that this continuous feedback law has been constructed by estimating $d\nu$ at each instant of time. The feedback law depends on **P**, **S**, and **V** as functions of time. A particular advantage of the sweepback method is the solution of $P(t_0)$, $S(t_0)$, and $V(t_0)$, allowing the guidance law to store these values and propagate them forward to the current time to calculate the current feedback gain. Propagation of the feedback gain may be by integration or more practically by interpolation between stored values. Use of this control should keep the trajectory on a neighboring optimal solution and deliver the spacecraft to the required orbit in the specified transfer time.

If the transfer time is not fixed, and was chosen optimally for the nominal trajectory. Then the formulation for free final time as stated earlier can be used to obtain the feedback guidance law

$$\delta\theta(t) = -H_{\theta\theta}^{-1}\left[\left(f_u^T\overline{P}\right)\delta x + f_u^T\overline{S}dv\right]$$
$$= -H_{\theta\theta}^{-1}\left[f_u^T\left(-\overline{S}\overline{V}^{-1}\overline{S}^T\right)\right]\delta x \tag{74}$$

and the change in the final time, dt_f, is:

$$dt_f = -\left[\left(\frac{\mathbf{m}^T}{\alpha} - \frac{\mathbf{n}^T}{\alpha}\overline{V}^{-1}\overline{S}^T\right)\right]\delta x \tag{75}$$

Evaluating dt_f determines when the thrust will be turned off to complete the transfer.

The block diagram for the feedback controller needed for neighboring optimal feedback guidance is shown in Figure 16.

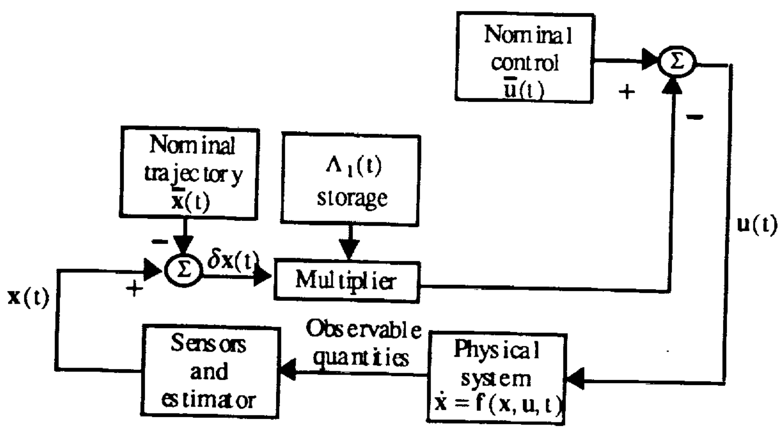

Figure 16: Diagram of Neighboring Optimal Feedback Controller Implementation. [13]

In Figure 16 $\Lambda_1(t)$ is the feedback gain for the $\delta\theta$ equation.

To determine when the new switching times should be, a variation of the switching function must be taken

$$d\mathbf{H}_T = \mathbf{H}_{Tx}dx + \mathbf{H}_{T\lambda}d\lambda + \mathbf{H}_{T\theta}d\theta = 0 \tag{76}$$

Therefore, the equation to find the change in the switching time is

$$dt_s = \frac{-\mathbf{H}_{Tx}\delta\mathbf{x} - \mathbf{H}_{T\lambda}\delta\lambda - \mathbf{H}_{T\theta}\delta\theta}{\mathbf{H}_{Tx}\dot{\mathbf{x}} + \mathbf{H}_{T\lambda}\dot{\lambda} + \mathbf{H}_{T\theta}\dot{\theta}} = \frac{\partial\left(\dot{\lambda}^{\mathrm{T}}\delta\mathbf{x} - \dot{\mathbf{x}}^{\mathrm{T}}\delta\lambda\right)/\partial T}{\partial\left(-\dot{\lambda}^{\mathrm{T}}\dot{\mathbf{x}} - \dot{\mathbf{x}}^{\mathrm{T}}\dot{\lambda}\right)/\partial T}$$
$$= \frac{\dot{\lambda}^{\mathrm{T}}\delta\mathbf{x} - \dot{\mathbf{x}}^{\mathrm{T}}\delta\lambda}{-2\dot{\mathbf{x}}^{\mathrm{T}}\dot{\lambda}} \tag{77}$$

In order to implement changes in the switching times it will be necessary to predict future errors in the state. The state transition matrix should be sufficient in this matter. Such predictions will provide the foresight to make switching times earlier or later when necessary.

V. Simulation Results For The Free Final Time Solution Using The One Burn Case

The controller was implemented by simulating the one burn case for the free final time solution. The simulation corresponds to a forward integration of the states, costates, and the assumed variables, **P**, **S**, **V**, **m**, **n**, and α from the initial time to the final time.

A comparison of the nominal and actual trajectories is shown in Fig. 17. (The actual trajectory being that generated from the simulation results.) Fig. 18 shows a plot of the actual and approximated errors in the trajectories when each state is perturbed from a value of 10^{-4} (actual refers to the difference between the nominal and actual trajectories and approximated refers to the integrated error). It is seen that the actual and approximated errors are concurrent with one another; however, they do not approach zero which implies that stability in this case is not guaranteed. Figure 19 shows the approximated error during the backward integration in which the error at the final time as set to a small number. This plot seems to show a stable response. In order to examine response on a more general basis, the 2-norm of the system transition matrix was plotted in Fig. 20. Obviously, if the 2-norm went to zero, response to initial conditions would be stable. By this plot, it would seem that in general the response will not be decreasing.

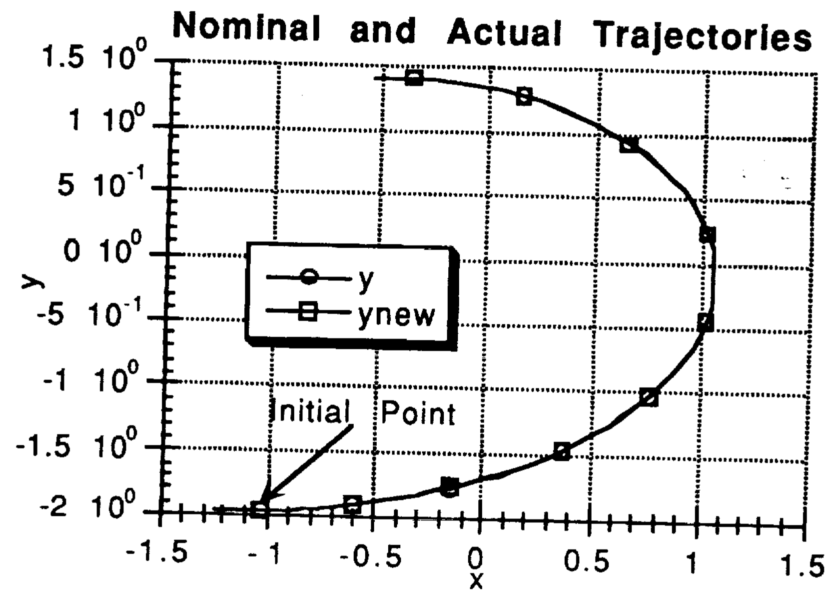

Figure 17: Plot of the Nominal and Actual Trajectories.

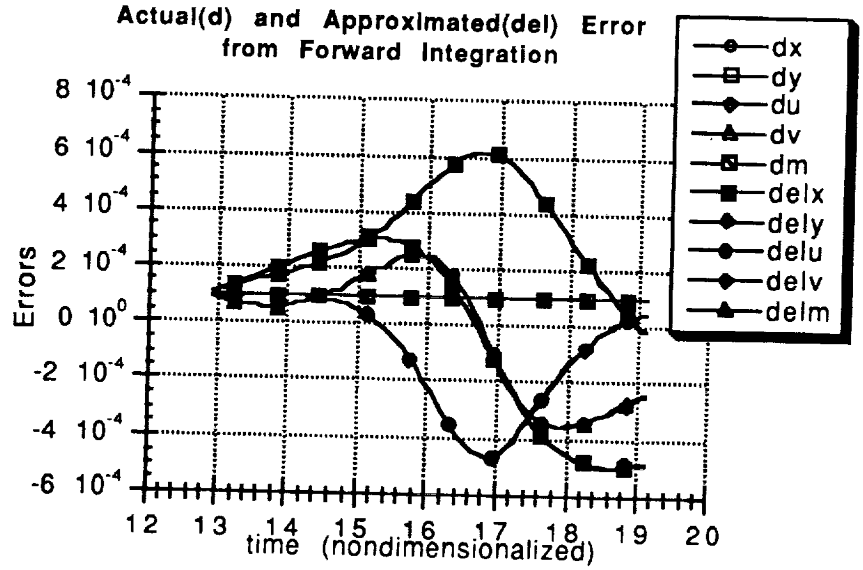

Figure 18: Plot of the Actual and Approximated Errors.

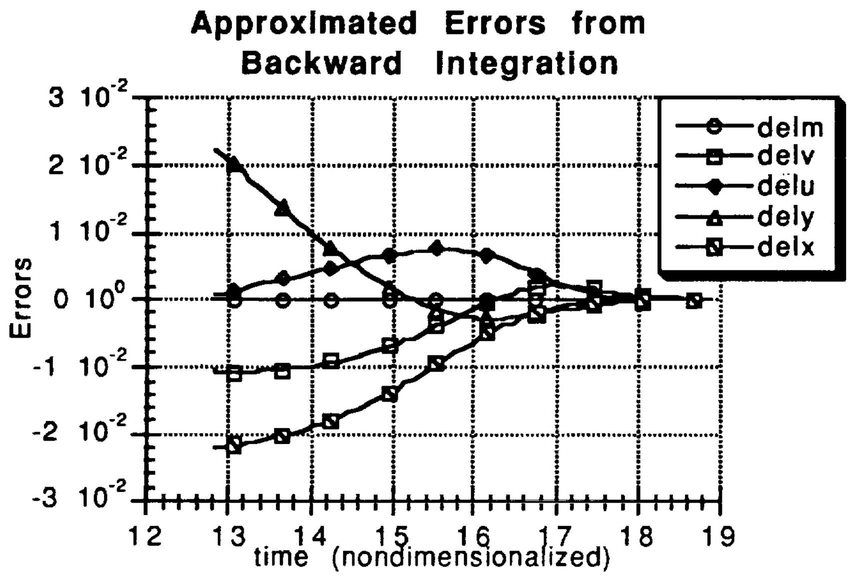

Figure 19: Plot of the Approximated Errors for Backward Integration.

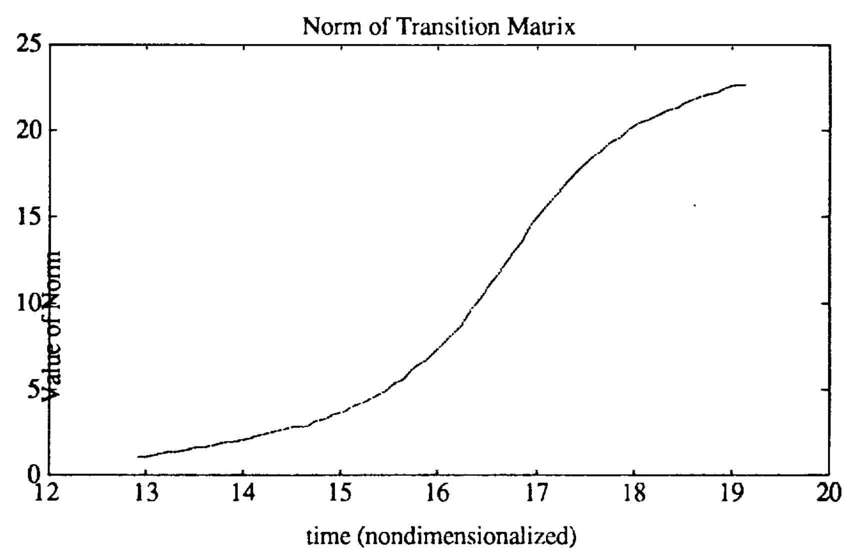

Figure 20: Plot of the Norm of the Transition Matrix.

VI. Patched Transfer Method Progress

Recent work in this research project has been directed toward developing a numerical computation scheme that performs well for a wide range of acceleration levels and target parameters. Current effort is in assembling a method referred to here as the Patched Method.

The Patched Method is to consist of two phases: a transfer orbit optimization phase and a orbit transfer solver phase. The transfer orbit optimization phase is not so much concerned with what values of the Lagrange multipliers are required to take the craft from orbit A to orbit B as it is with how much time or fuel is required. The orbit transfer solver phase, however, is more concerned with obtaining an accurate representation of the transfer and is equally concerned with the values of the Lagrange multipliers as it is with the transfer time. Finally, it also seems reasonable to desire a method that will search for the optimal solution satisfying the target parameters but will also, if that fails, be able to return a sub-optimal solution satisfying the target parameters. In other words, it would be better to calculate a sub-optimal solution than obtain no solution at all.

Obviously, the key algorithm is one that can quickly determine the minimum transfer time (and fuel requirement) between two given orbits in a single burn. One approach that may give satisfactory results is an application of multivariate interpolation. Interpolation requires calculation and storage of data ahead of time. Therefore, the first question is what needs to be stored? To completely specify a problem the following twelve (12) values are required: semimajor axis $a(t_o)$ and $a(t_f)$, eccentricity $e(t_o)$ and $e(t_f)$, true anomaly $\nu(t_o)$ and $\nu(t_f)$, argument of perigee $\omega(t_o)$ and $\omega(t_f)$, mass $m(t_o)$, thrust T, specific impulse I_{sp}, and transfer time, t_f. To specify the problem's solution storage of the Lagrange multipliers $\lambda_x(t_o)$, $\lambda_y(t_o)$, $\lambda_u(t_o)$, $\lambda_v(t_o)$, $\lambda_m(t_o)$ is required.

The first of the nondimensionalization equations, Eqn. [23], says that $a(t_o)$ can be set to unity ($a(t_o)$=1) for any orbit transfer problem. A simple choice of coordinate axis, aligning it with perigee, will set the initial argument of perigee to be set to zero degrees, which also works for any orbit transfer problem. Neither eccentricity nor true anomaly have such favorable scaling qualities. Additionally, now that the initial values have been scaled, the final values cannot. The influence of specific impulse can be removed by assuming a constant mass. The mass may be corrected at the end of the burn, so that calculation of the following burn is more accurate. Assuming constant mass also removes the need to store λ_m.

The influence of the thrust level may be removed by a somewhat restrictive assumption, $(\delta r/\rho)^2 << 1$, where δr is distance between the actual position of the craft and a point on a reference orbit with current radius ρ. This assumption is consistent both with low thrust levels, which stay close to a reference orbit for several revolutions, and medium thrust levels, which may only stay close to a reference orbit for a few revolutions. The advantage is that the assumption linearizes the dynamics and allows the solution to be written as

$$\begin{bmatrix} \delta \mathbf{r}(t) \\ \delta \mathbf{v}(t) \end{bmatrix} = \Phi(t,t_o) \begin{bmatrix} \delta \mathbf{r}(t_0) \\ \delta \mathbf{v}(t_0) \end{bmatrix} + T \int_{t_0}^{t} \left[\frac{\Phi(t,\tau)}{m(\tau)} \begin{bmatrix} 0 \\ e_T(\tau) \end{bmatrix} \right] d\tau \qquad (78)$$

Where $\Phi(t,t_o)$ is the state transition matrix for the homogeneous solution. If the initial conditions are set to zero, then the solution is linear with respect to the thrust. Now, one solution can easily be scaled for any thrust level; however, the resulting solution must satisfy the assumption. The orbital elements can then be determined using a Jacobian matrix, as shown in Eq. [79] and easily obtained by taking partial derivatives of equations used to convert Cartesian coordinates to orbital elements.

$$\begin{bmatrix} \delta a \\ \delta e \\ \delta v \\ \delta \omega \end{bmatrix} = \mathbf{J}(a_o, e_o, v_o, \omega_o) \begin{bmatrix} \delta \mathbf{r} \\ \delta \mathbf{v} \end{bmatrix} \qquad (79)$$

The number of parameters required to specify a given transfer are reduced to seven (7): $\delta a(t_f)$, $e(t_o)$, $\delta e(t_f)$, $\delta \omega(t_f)$, $v(to)$, $\delta v(t_f)$, and t_f; the transfer time stored with this data is the minimum time required for the transfer. To store the solution, it is still required to know all the Lagrange multipliers.

Before proceeding much further with this discussion a few words should be said about multivariate interpolation. It is assumed the reader is familiar with univariate, or single variable, interpolation in which there is only one independent variable and one scalar function of that variable, though any number of such dependent variables is allowed. Bivariate interpolation is then interpolation involving two independent variables and at least one function of these variables. Bivariate interpolation, and this applies equally well to multivariate interpolation, is most easily implemented when the values for independent variables are evenly spaced in a grid[14].

However, in the case of orbital transfer it would be quite difficult to obtain data with the orbital elements of the target orbit evenly spaced because this would require an iterative solver for each data point. If that process were easy, there would be no need for this approach. On the other hand, it is relatively easy to obtain a grid with the Lagrange multipliers, orbital elements of the initial orbit, and the transfer time evenly spaced. The equations of motion can then be integrated and the orbital elements of the destination orbit are known. The difficulty associated with the unevenly spaced grid is evident when one has values for the elements of the target orbit and wants to obtain the values of the Lagrange multipliers and the required transfer time. Currently, both types of grids are being considered.

The spacing of the grid is another issue altogether. The spacing of the grid, or its density, will determine the accuracy of the estimated minimum transfer time. Since speed of the algorithm and storage space required for the software are always important, the grid will need a somewhat wide spacing. There are 7 values to store for each point in the grid; whichever of the other 4 variables are evenly spaced, it is easy to determine their values though proper indexing of the grid points. If each variable is allowed n different values and 8 bytes are used to store each number in the computer, then the grid will occupy $56n^7$ bytes of memory. For the grid to need under one megabyte of space, then n=4 is required. For n=5, the grid would occupy just over 4 megabytes of space. More than likely, different spacings of each variable would be most efficient but will this will not change the fact that the grid cannot be dense.

This interpolation will most surely produce a quick, though rough estimate of the transfer time between two chosen orbits. The next phase of the method is to obtain accurate solutions for the transfers between these orbits. Estimates for the Lagrange multipliers can be also obtained through the interpolation. These can then be used as an initial guess for a numerical solver. And, if that fails, a homotopy algorithm can be initiated from a nearby grid data point since that data point is already an accurate solution.

VII. Conclusions

Concerning the calculation of optimal transfers, the current direction has been elaborated upon, which is to test numerical methods within the framework of the Patched Method. Some work from previous reports and borrowing techniques from the literature will be incorporated along with the discussed methods. Results from this work are forthcoming.

A few conclusions, which lend themselves to study in current research work, can be made from the analyses presented here. If there are no algorithm mistakes, then it can be concluded that the extremal solutions examined may not be locally optimal solutions for fixed transfer time. However, some considerations necessary for an accurate examination of the second variation may have been overlooked. Ongoing research work is in examining why these conditions are not met.

It was found that the sufficient conditions were satisfied for the free final time problem. Software has been developed in order to simulate neighboring optimal feedback guidance. Currently, this software is not producing stable solutions. The issue of stability of the response must be investigated further and is an area of current research endeavors.

VIII. REFERENCES

[1]Brusch, R.G. and Vincent, T.L., "Low-Thrust, Minimum-Fuel, Orbital Transfers," *Astronautica Acta*, Vol. 16, pp 65-74.

[2]Edelbaum, T.N., Sackett, L.L., and Malchow, H.L.., "Optimal Low Thrust Geocentric Transfer" *AIAA Paper 73-1074, AIAA 10th Electric Propulsion Conference, Lake Tahoe, Nevada, November 1973*

[3]Redding, D.C., "Optimal Low-Thrust Transfers to Geosynchronous Orbit," NASA Lewis SUDAAR 539, Cleveland, Ohio 44135, Sept. 1983.

[4]Zondervan, K.P., Lincoln, L.J., And Caughey, T.K., "Optimal Low-Thrust, Three-Burn Orbit Transfers with Large Plane Changes," *Journal of the Astronautical Sciences*, Vol. 32, No. 3, 1984, pp. 407-427.

[5]Anderson, G.M., and Smith, E.A., "A Combined Gradient/Neighboring Extremal Algorithm for the Calculation of Optimal Transfer Trajectories between Noncoplanar Orbits using a Constant Low Thrust Rocket," *Journal of the Astornautical Sciences*, Vol. 23, No. 3, 1984, pp. 225-239

[6]Smith, I. E. "General Formulation of the Iterative Guidance Mode," Technical Memorandum X-53414, NASA-George C. Marshall Space Flight Center, March 22, 1966.

[7]Lu, P. "A General Nonlinear Guidance Law...," Guidance, Navigation, and Control Conference, Scottsdale, Arizona, 1994.

[8]Hough, Michael E. "Explicit Guidance Along an Optimal Space Curve," *Journal of Guidance, Control, and Dynamics.* Vol. 12, 1989, pp.495-504.

[9]Tempelman, Wayne. "Linear Guidance Laws for Space Missions," *Journal of Guidance, Control, and Dynamics.* Vol. 9, 1986, pp,495-502.

[10]Naidu, D. Subbaram. *Aeroassisted Orbital Transfer: Guidance and Control Strategies.* New York: Springer-Verlag, 1994.

[11]Powers, William F. "Techniques for Improved Convergence in Neighboring Optimal Guidance," *AIAA Journal.* Vol. 8, 1970, pp. 2235-2241.

[12]Chuang, C.-H., Goodson, T.D., and Hanson, J. "Optimal Trajectories of Low- And Medium-Thrust Orbit Transfers with Drag and Oblateness," submitted to *Journal of the Astronautical Sciences*, 1994

[13]Bryson, A.E., and Ho, Y.-C., *Applied Optimal Control.* Philadelphia: Taylor and Francis, 1975.

[14]Press, W.H., Flannery, B.P., Teukolsky, S.A., and Vetterling, W.T. *Numerical Recipes.* New York: Cambridge University Press, 1990.